



OPEN ACCESS

EDITED BY

Philippe Sucosky,
Kennesaw State University, United States

REVIEWED BY

Yanina Zócalo,
Centro Hospitalario Pereira Rossell
(University of the Republic), Uruguay
Ricardo Armentano,
Universidad de la República, Uruguay

*CORRESPONDENCE

Vasiliki Bikia,
✉ vasiliki.bikia@epfl.ch

RECEIVED 03 April 2023

ACCEPTED 15 May 2023

PUBLISHED 30 May 2023

CITATION

Bikia V, Rovas G and Stergiopoulos N
(2023), Cardiac output estimated from an
uncalibrated radial blood pressure
waveform: validation in an *in-silico*-
generated population.
Front. Bioeng. Biotechnol. 11:1199726.
doi: 10.3389/fbioe.2023.1199726

COPYRIGHT

© 2023 Bikia, Rovas and Stergiopoulos.
This is an open-access article distributed
under the terms of the [Creative
Commons Attribution License \(CC BY\)](#).
The use, distribution or reproduction in
other forums is permitted, provided the
original author(s) and the copyright
owner(s) are credited and that the original
publication in this journal is cited, in
accordance with accepted academic
practice. No use, distribution or
reproduction is permitted which does not
comply with these terms.

Cardiac output estimated from an uncalibrated radial blood pressure waveform: validation in an *in-silico*-generated population

Vasiliki Bikia*, Georgios Rovas and Nikolaos Stergiopoulos

Laboratory of Hemodynamics and Cardiovascular Technology, Institute of Bioengineering, Swiss Federal Institute of Technology, Lausanne, Switzerland

Background: Cardiac output is essential for patient management in critically ill patients. The state-of-the-art for cardiac output monitoring bears limitations that pertain to the invasive nature of the method, high costs, and associated complications. Hence, the determination of cardiac output in a non-invasive, accurate, and reliable way remains an unmet need. The advent of wearable technologies has directed research towards the exploitation of wearable-sensed data to improve hemodynamical monitoring.

Methods: We developed an artificial neural networks (ANN)-enabled modelling approach to estimate cardiac output from radial blood pressure waveform. *In silico* data including a variety of arterial pulse waves and cardiovascular parameters from 3,818 virtual subjects were used for the analysis. Of particular interest was to investigate whether the uncalibrated, namely, normalized between 0 and 1, radial blood pressure waveform contains sufficient information to derive cardiac output accurately in an *in silico* population. Specifically, a training/testing pipeline was adopted for the development of two artificial neural networks models using as input: the calibrated radial blood pressure waveform (ANN_{calradBP}), or the uncalibrated radial blood pressure waveform (ANN_{uncalradBP}).

Results: Artificial neural networks models provided precise cardiac output estimations across the extensive range of cardiovascular profiles, with accuracy being higher for the ANN_{calradBP}. Pearson's correlation coefficient and limits of agreement were found to be equal to [0.98 and (−0.44, 0.53) L/min] and [0.95 and (−0.84, 0.73) L/min] for ANN_{calradBP} and ANN_{uncalradBP}, respectively. The method's sensitivity to major cardiovascular parameters, such as heart rate, aortic blood pressure, and total arterial compliance was evaluated.

Discussion: The study findings indicate that the uncalibrated radial blood pressure waveform provides sample information for accurately deriving cardiac output in an *in silico* population of virtual subjects. Validation of our results using *in vivo* human data will verify the clinical utility of the proposed model, while it will enable research applications for the integration of the model in wearable sensing systems, such as smartwatches or other consumer devices.

KEYWORDS

arterial pulse wave, vascular age, non-invasive monitoring, neural networks, cuff-free

Introduction

Cardiac output (CO) is defined as the volume of blood expelled by the left ventricle per unit time. Critically ill patients generally have abnormal oxygen demands as a result of the underlying diseases. Thus, CO monitoring is essential for patient management in the operating room and the intensive care unit (ICU) (Berkenstadt et al., 2001; Lees et al., 2009). Direct methods for measuring CO include invasive approaches, such as the Fick method and the thermodilution method. Alternative approaches, such as pulse contour analysis (Udy et al., 2012), have been put forth as less invasive methods. However, pulse contour analysis necessitates the placement of a pressure catheter at an arterial site (Jansen et al., 2001; Udy et al., 2012; Ganter et al., 2016).

On the other hand, non-invasive methods for CO have been introduced in order to overcome the complications and potential risk of the invasive and minimally invasive techniques. Some non-invasive methods are based on pulse wave analysis from the cross-sectional area and blood velocity data (Segers et al., 2007) or directly from MRI-derived aortic flow-time signals (Hickson et al., 2010). Doppler ultrasound and MRI, while completely non-invasive and reasonably accurate, require the allocation of expensive resources. It is of interest to mention that a previous study (Zócalo et al., 2021) investigated the impact of sex, age, heart rate, and anthropometric characteristics on the estimation of stroke volume, CO, and cardiac index in a large cohort of 1,449 healthy subjects covering a wide range of age values (3–88 years). CO was non-invasively obtained based on pulse contour analysis (PCA) on brachial BP acquired using the Mobil-O-Graph device (Mobil-O-Graph; Germany). Importantly, the study demonstrated that gender, age, heart rate, and body surface area are independent factors that explain PCA-derived CO values, suggesting that they should be taken into account in CO monitoring applications. Moreover, impedance cardiography (ICG) provides another rather clinically relevant alternative to monitor stroke volume and CO, allowing for the assessment of these parameters during both stress conditions and at rest (Liu et al., 2021). Yet, none of the aforementioned methods are practical for continuous bedside monitoring of a patient's CO or routine examination. As a result, the determination of CO in a non-invasive, accurate, and reliable way remains an unmet need.

Recent advances in measuring sensors have spurred the development of a gamut of methods to calculate CO from arterial blood pressure (BP) signals, with many of them being commercially available. The main aspects that have encouraged this approach include: (i) the fact that arterial BP can be acquired in a relatively easy, non-invasive (or minimally invasive), and cost-effective manner; (ii) arterial BP is measured in clinical settings such as ICUs on a routine basis; and (iii) the arterial BP is measured continuously, allowing for continuous CO estimates. In addition, the advent of wearable technologies has enabled research efforts towards the exploitation of wearable-sensed data to improve hemodynamical

monitoring. Especially, smartwatches and fitness bands can provide access to peripheral arterial pulse waves, which could be afterwards further analyzed in order to provide major hemodynamic parameters, such as arterial stiffness, cardiac output, etc.

In this study, we introduced a novel machine learning-enabled method to estimate CO from radial BP waveform. Given that simultaneous invasive radial BP and CO data are typically difficult to acquire *in vivo*, we leveraged a previously generated *in silico* dataset simulating 3,818 virtual subjects (Bikia et al., 2021). A training/testing pipeline using artificial neural networks (ANN) was adopted for the development of two ANN models using as an input vector: (i) the calibrated radial BP waveform, or (ii) the uncalibrated radial BP waveform. The performance of the resulted predictive models was evaluated by comparing the model-derived values with the reference CO data.

Materials and methods

In silico population

In this study, we used an *in silico* dataset from our previously published work (Bikia et al., 2021). The data generation relied on a previously developed, clinically validated one-dimensional cardiovascular computer simulator (Reymond et al., 2009) and intended to emulate the content of various hemodynamical profiles. The cardiovascular model (Reymond et al., 2009) ran using different combinations of input model parameters based on publicly available literature data which were varied using a random Gaussian distribution. The parameters of arterial distensibility, terminal compliance, and peripheral resistance were altered in

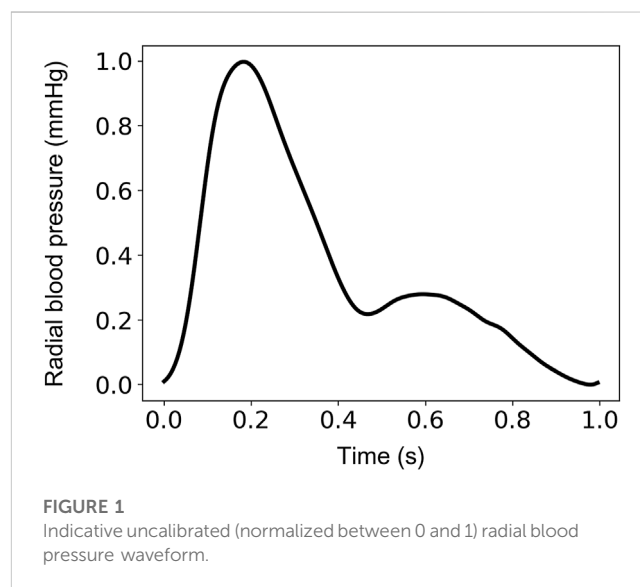


TABLE 1 Description of the artificial neural networks-based models.

Model	Input	Batch size	Selected number of epochs
ANN _{calradBP}	Calibrated radial blood pressure waveform	64	61
ANN _{uncalradBP}	Uncalibrated radial blood pressure waveform	64	71

TABLE 2 Description of the cardiovascular parameters of the *in silico* data.

Parameter	<i>In silico</i> population <i>n</i> = 3,818		
	Min	Max	Mean ± SD
Aortic systolic BP (mmHg)	77	187	123 ± 24
Aortic diastolic BP (mmHg)	43	128	80 ± 21
Aortic pulse pressure (mmHg)	11	106	42 ± 19
Mean arterial pressure (mmHg)	66	155	101 ± 21
Radial systolic BP (mmHg)	85	193	133 ± 23
Radial diastolic BP (mmHg)	37	119	73 ± 21
Radial pulse pressure (mmHg)	21	124	60 ± 22
Heart cycle (s)	0.6	1	0.7 ± 0.1
Total peripheral resistance (mmHg.s/mL)	0.6	1.4	1 ± 0.2
Total arterial compliance (mL/mmHg)	0.3	2.9	1.1 ± 0.5
Cardiac output (L/min)	3.3	10.5	6 ± 1.2

order to achieve the specific value in the selected ranges. Furthermore, the length, inlet diameter, and outlet diameter of every arterial segment was modified to simulate different body types by adapting the length and the diameter of all arterial vessels. The reader is referred to the original publication (Bikia

et al., 2021) for the detailed description of the data design and generation.

The simulated radial BP waveform was derived from the virtual left radial artery. In addition, *in silico* BP values, such as the mean arterial pressure, systolic and diastolic BP, and pulse pressure at the aortic root became available from the model-simulated aortic BP waveform. CO was calculated as the product of heart rate and stroke volume, which was calculated from the area under the curve of the aortic blood flow rate. Values of total arterial compliance were derived analytically by summing the incremental volume compliance of all arterial segments. The data were organized in input-output pairs for every virtual subject, namely, the radial BP waveform and the respective CO value were assigned to every virtual subject.

Data analysis

The input-output sets were subsequently divided into train, validation, and test sets. The train/validation/test split was set to be 60% (2,290 cases)/20% (764 cases)/20% (764 cases). The sampling frequency was set to 128 Hz. This selection allowed us to ensure a sampling frequency higher than the 100-Hz threshold suggested for the pulse wave velocity techniques (Gaddum et al., 2013) (which require substantially high temporal resolution). This value was considered as a fair trade-off between computational time and high signal fidelity. Normalization of the radial BP waveforms was performed between 0 and 1 using the linear scaling

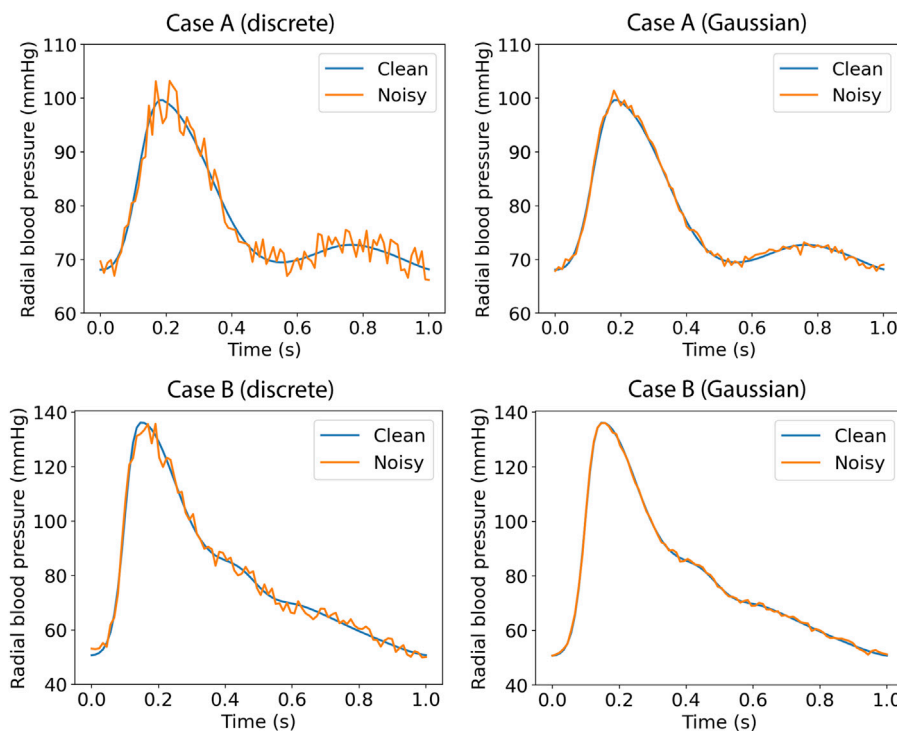


FIGURE 2 Radial blood pressure data with added artificial random noise.

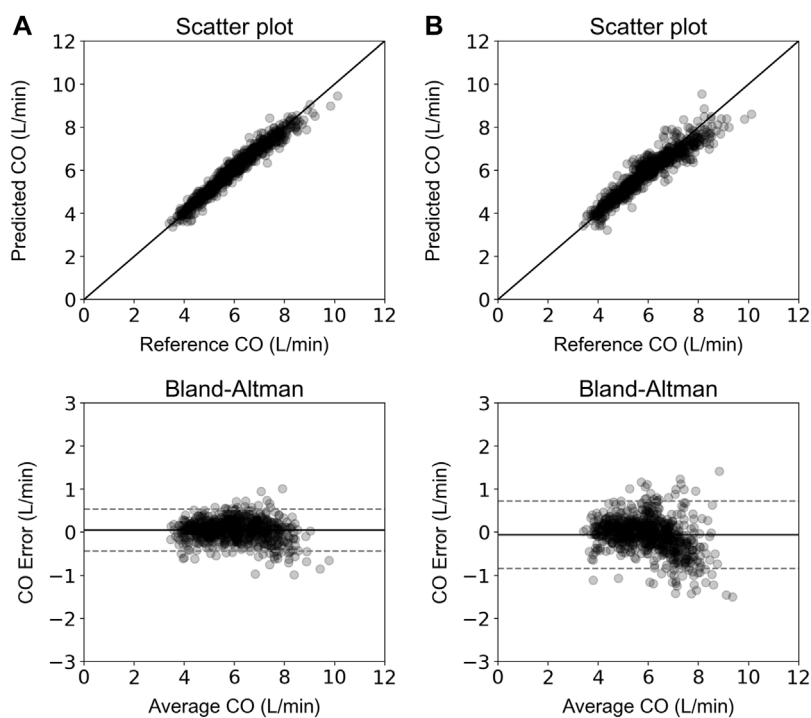


FIGURE 3

Scatter plot and Bland-Altman analysis between the estimated and reference CO values for the ANN_{calradBP} (A) and ANN_{uncalradBP} (B). The solid line of the scatterplots represents equality. In Bland-Altman plots, the solid black line represents the bias and the two horizontal dashed lines define the limits of agreement (LoA), within which 95% of errors are expected to lie.

formulation. An indicative example of an uncalibrated radial BP waveform normalized between 0 and 1 is shown in Figure 1.

Artificial neural networks model

We used artificial neural networks (ANN) to estimate the target variable of interest, namely, CO. For the ANN, a fixed one-hidden layer structure was selected and the “Adam” optimizer was used (Kingma and Jimmy, 2017). A training/testing pipeline was adopted for the development of two ANN models using as an input vector: (i) the calibrated radial BP waveform (ANN_{calradBP}), or (ii) the uncalibrated radial BP waveform (ANN_{uncalradBP}). Subsequently, the performance of the trained predictive models was evaluated by comparing the model-derived values with the reference CO data.

To mitigate overfitting and to increase the generalization capacity, machine learning models should be trained for optimal hyperparameter values. For the ANN, the batch size (defines the number of samples that will be propagated through the network) was set to be equal to 64, whereas the number of epochs was optimized. The number of epochs defines the number of times that the learning algorithm works through the entire training data set. For selecting the optimal value of epochs, we computed the training loss and the validation loss for various values of epochs. Loss values (using the mean squared error method) were

monitored by an early-stopping call-back function. When an increment is observed in the loss values, training comes to an halt and the respective value of epoch indicates the optimal selection. Description of the ANN-based models and the selected number of epochs that was computed are presented in Table 1. Subsequently, the test set was fed into the trained models to predict CO and the precision was evaluated. The training/testing pipeline as well as the pre-analyses and post-analyses were implemented using the Scikit-learn library (Pedregosa et al., 2011) in a Python programming environment. The Pandas and Numpy packages were used (Oliphant, 2006; McKinney, 2010).

In silico data cannot simulate different aspects that usually occur with real data registries (e.g., imperfection of signals, over-damping, etc.). In order to assess the performance of the proposed method on input signals with errors or other imperfections, we tested the ANN models (using the same model configuration) after artificially adding random noise. Firstly, we selected a more brute-force scenario where the error for each pressure data point was randomly drawn from the range of $\pm 5\%$. Each pressure data point was multiplied with a random noise factor; for instance, for a randomly selected error of -3% , the respective variable value was multiplied with a noise factor equal to 0.97. Secondly, to simulate more realistic measurement errors, we added artificial random noise assuming a Gaussian distribution with $\mu = 0.7$ mmHg, and $SD = 1$ mmHg. Indicative examples of the noisy data are shown in Figure 2.

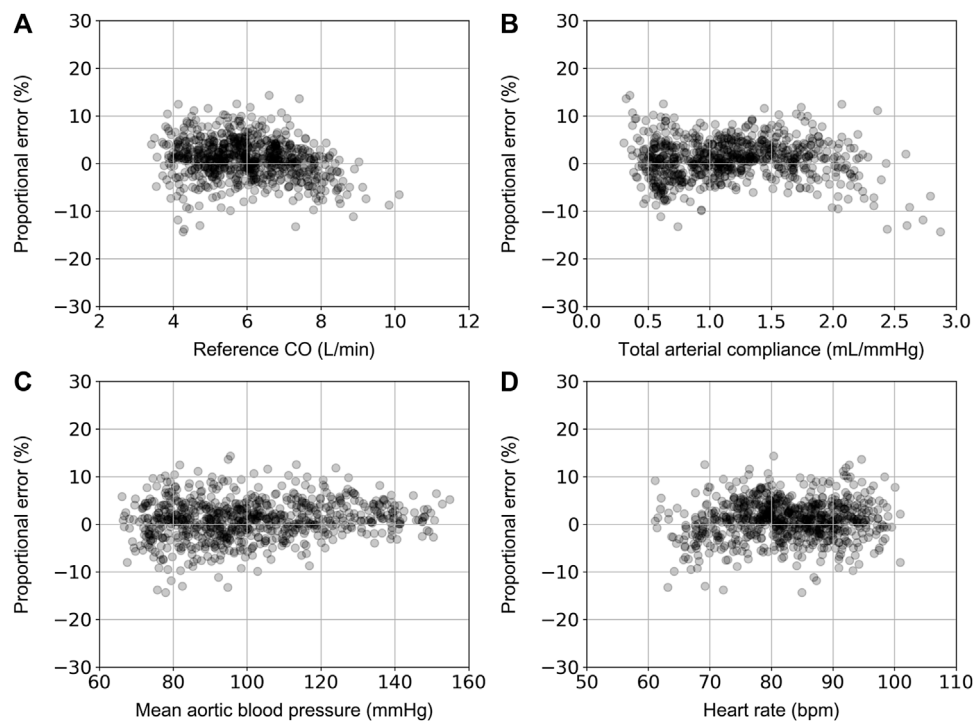


FIGURE 4 Comparison of proportional error, calculated as $CO_{\text{predicted}} - CO_{\text{reference}} / CO_{\text{reference}}$, with reference CO (A), total arterial compliance (B), mean aortic blood pressure (C), and heart rate (D).

Statistical analysis

All data are presented as mean and standard deviation (SD). The statistical analysis was performed in Python (Python Software Foundation, Python Language Reference, version 3.6.8, available at <http://www.python.org>). The correlation and precision between the estimations and the reference data were evaluated using the Pearson’s correlation coefficient (*r*), and the normalized root mean square error (nRMSE). The computed

nRMSE was based on the difference between the minimum and maximum values of the dependent variable (*y*) and was computed as $RMSE / (y_{\text{max}} - y_{\text{min}})$. Bias and limits of agreement (LoA) (where the 95% of errors are expected to lie) were calculated using the Bland-Altman analysis (Bland and Altman, 1986). Linear least-squares regression was performed for the estimated and reference data. The slope and the intercept of the regression line were reported. Two-sided *p*-values for hypothesis tests were calculated using Wald Tests with t-distribution of the test statistic. The null

TABLE 3 Accuracy, agreement, and correlation between ANN-predicted and reference CO data.

Model	<i>r</i>	MAE (L/min)	nRMSE (%)	Bias (LoA) (L/min)	Reference CO (L/min)	Estimated CO (L/min)	Slope/Intercept
ANN _{calradBP} (no noise)	0.98	0.19	3.7	0.05 (−0.44, 0.53)	6 ± 1.2	6 ± 1.2	0.95 (<i>p</i> < 0.0001)/ 0.32 L/min
ANN _{calradBP} (discrete)	0.95	0.28	5.7	−0.03 (−0.74, 0.68)	5.8 ± 1.2	5.8 ± 1.2	0.95 (<i>p</i> < 0.0001)/ 0.25 L/min
ANN _{calradBP} (Gaussian)	0.97	0.34	6	−0.28 (−0.84, 0.28)	6 ± 1.2	5.7 ± 1.1	0.91 (<i>p</i> < 0.0001)/ 0.26 L/min
ANN _{uncalradBP} (no noise)	0.95	0.3	6	−0.06 (−0.84, 0.73)	6 ± 1.2	5.9 ± 1.1	0.85 (<i>p</i> < 0.0001)/ 0.84 L/min
ANN _{uncalradBP} (discrete)	0.77	0.69	12.3	0.13 (−1.56, 1.83)	6.1 ± 1.3	6.2 ± 1.3	0.79 (<i>p</i> < 0.0001)/ 1.39 L/min
ANN _{uncalradBP} (Gaussian)	0.88	0.45	8.6	−0.02 (−1.17, 1.12)	6 ± 1.2	5.9 ± 1.1	0.78 (<i>p</i> < 0.0001)/ 1.29 L/min

r, Pearson’s correlation coefficient; MAE, mean absolute error; nRMSE, normalized root mean square error; LoA, limits of agreement.

hypothesis was that the slope is zero. A $p < 0.05$ was considered statistically significant.

Results

Table 2 aggregates the cardiovascular parameters of the *in silico* data ($n = 3,818$). Comparison between the model-derived predictions and the reference data was performed. Accuracy was reported to be increased for the ANN model that used the calibrated radial BP waveform as an input ($r = 0.98$). In both models, LoA were narrow and biases were found to be close to zero. The scatter plots and the Bland–Altman plots of the estimated CO for the two ANN models against the ground truth are shown in Figure 3. For the ANN models using the noisy data as input, the accuracy was lower with increasing level of assumed noise. The ANN_{calradBP} was found to be more robust to the addition of random noise in comparison to the ANN_{uncalradBP}. Overall, correlation values between the estimated and reference CO data remained at satisfactory levels (≥ 0.77). In the case of ANN_{calradBP}, nRMSE values were low ($\leq 6\%$). The nRMSE was essentially increased in ANN_{uncalradBP}, especially when discrete random noise was added to the signals (nRMSE was doubled). All regression metrics for the agreement, precision, and bias are presented in Table 3.

For the ANN_{calradBP}, the proportional error (PE) with respect to the reference CO values is shown in Figure 4. The

PE was calculated as $(CO_{\text{predicted}} - CO_{\text{reference}})/CO_{\text{reference}}$. The maximum and minimum PE values were reported to be 14.4% and -14.3% , respectively. In addition, the distribution of PE was found to be equal to $0.9\% \pm 4.1\%$. The respective values for the ANN_{uncalradBP} were the following: $PE_{\text{max}} = 22.6\%$, $PE_{\text{min}} = -25.6\%$, $PE_{\text{mean}} = -0.5\%$, and $PE_{\text{SD}} = 6.3\%$ (Figure 5). The PE demonstrated an increasing trend with increasing CO values. No correlation was reported for the PE resulted from both ANN_{calradBP} and ANN_{uncalradBP} models with respect to heart rate, total arterial compliance, and mean aortic blood pressure (Figures 3, 4).

Discussion

This article introduced an ANN-enabled method to estimate CO from the radial BP waveform. In particular, we investigated the concept of deriving CO from, firstly, the calibrated radial BP waveform and, secondly, the morphology of the raw uncalibrated radial BP wave using an in-silico-generated virtual population of various hemodynamical profiles. The findings indicated that CO can be precisely predicted by exploiting the radial (peripheral) BP pulse wave. This method relies on the raw information hidden in the radial pulse wave that can be deciphered via the predictive capacity of neural networks with relatively simple structure. Ultimately, potential use of such methods could include the expansion and integration of a prediction algorithm to estimate CO using wearable sensing technologies (such as smartwatches or fitness trackers),

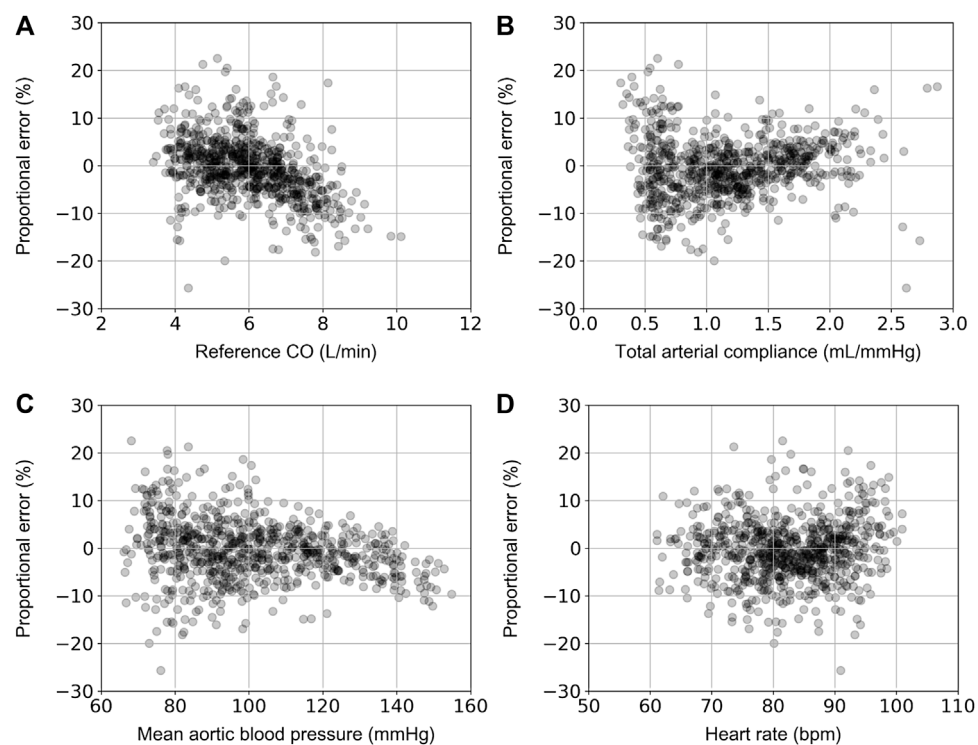


FIGURE 5

Comparison of proportional error, calculated as $(CO_{\text{predicted}} - CO_{\text{reference}})/CO_{\text{reference}}$, with reference CO (A), total arterial compliance (B), mean aortic blood pressure (C), and heart rate (D).

while eliminating the need for complex and expensive echocardiographic or MRI procedures.

Cardiac output (CO) is a key parameter in assessing circulatory function. Currently in clinical practice, the gold standard for CO measurement is thermodilution CO (TCO), which involves the insertion of a catheter into the pulmonary artery. Conducted primarily in ICUs, TCO is usually measured intermittently, is very invasive, and may cause severe complications. It would be a tremendous asset to healthcare if one could determine CO accurately, reliably, and continuously using less invasive, indirect methods. Over the last decades, numerous methodologies have been suggested and developed to estimate CO using peripheral arterial BP data obtained either minimally invasively or non-invasively (Sun et al., 2005; Litton and Morgan, 2012; Bikia et al., 2020a; Bikia et al., 2020b; Bikia, 2021; Saugel et al., 2021). Some of these estimators rely on elaborate models of the heart and vasculature while others use artificial intelligence methods such as pattern matching and classification trees. The majority of the published estimators has not been extensively evaluated with a large set of clinical arterial blood pressure data, hence their performance may need to be re-evaluated. An additional issue to be considered with regards to the validation of CO estimation techniques pertains to the establishment of universal, well-defined thresholds of acceptable accuracy. In contrast to the BP monitors, CO data from meta-analyses studies are limited, with only few and not up-to-date works trying to propose threshold of error values that could allow a newly introduced method to be considered as reliable, repeatable, and accurate (Critchley and Critchley, 1999; Critchley et al., 2014).

Typically, recording the calibrated radial BP waveform requires calibration using a conventional cuff procedure. At large, cuff-based devices have been widely used for non-invasive BP assessment and their utility is critical for several medical conditions (Tzourio et al., 2017). Nonetheless, there are various limitations in the use of methods relying on cuff-based BP measurement, including: i) low accuracy (Harris et al., 2016), ii) the measurement is usually intermittent and does not capture all BP changes occurring throughout the recording window, ii) and existing devices are bulky, not portable and thus not practical for daily use (O'Brien et al., 2013; Parati et al., 2014).

Many cuffless BP estimation methods have been proposed to overcome these limitations, enabling continuous BP monitoring (Kim et al., 2012; Kim et al., 2007; Baek, 2009), but not CO derivation. The tremendous majority of such methods is based on the pulse transit time (PTT) principle. PTT is the pulse wave propagation time, which represents the time required for the wave to travel between two arterial sites within the same cardiac cycle (Nye, 1964; Steptoe et al., 1976), and it is formally assessed in conjunction with a continuous electrocardiogram (ECG) (Geddes et al., 1981). The PTT indirectly depends on BP, as higher pressure results in a faster PTT (Geddes et al., 1981). While these methodologies could serve as a foundation for the development of similar CO estimation methods, conventional cuffless PTT-based estimation methods are still subject to cuff dependence as they necessitate at least one-time calibration.

A cuff-free, portable device that can measure CO without calibration would be valuable for continuous CO measurement, but it does not currently exist. Our analysis indicated that, in an *in silico* population generated from a numerical model of the

cardiovascular system, neural networks could enable the estimation of CO with the elimination of the calibration process, leading to a completely cuff-free solution. Such a solution will ultimately permit the integration of predictive models in wearable technologies. It is important to acknowledge that currently, smartwatches and fitness bands are not optimized to deliver precise and repeatable methods for recording pressure signals. However, the future holds promise (Liao et al., 2019), as sensing technologies continue to advance rapidly.

Undoubtedly, this study relies entirely on *in silico* data which, despite the high complexity of the adopted numerical model and the attentive design of the data generation, correspond to nearly perfect conditions. It is possible that there will be circumstances in real world clinical practice in which the *in silico* results may not be in line with the *in vivo* findings. Nevertheless, this model has undergone comprehensive validation in previous studies using *in vivo* data. Therefore, it can serve as an excellent starting point for evaluating the concept of cuff-free CO estimation, solely relying on the uncalibrated radial BP waveform as input. As gold-standard CO measurements require the use of invasive catheter-based procedures, it is worth verifying that the initial hypothesis is evaluated and validated *in silico*. Furthermore, we conducted tests on the proposed method while considering artificially introduced errors. This allowed us to assess its performance using data that could better simulate realistic data registries. Positive results, as those produced by this study, can now be the basis for extending the analysis on human data and investigating the validity of this method in the clinic. Of particular interest is to evaluate this method's accuracy in children's populations, as childhood hemodynamics differ inherently in comparison to adult hemodynamics [e.g., minimum levels of aortic systolic blood pressure may be equal to 60 mmHg (Zinoveev et al., 2019)]. Furthermore, as a next step, we intend to assess the model's performance in individuals performing low-, moderate-, or high-intensity physical activity. Yet, based on the sensitivity analysis of the prediction error, we demonstrated that the estimation error is not correlated to the value of mean aortic blood pressure and heart rate. Moreover, future work will include testing the accuracy of the proposed methodology using clinical data from both healthy subjects (controls) and patients with various forms of cardiovascular disease (especially in cases where the presence of extreme CO levels is possible). The latter will allow to evaluate the method's discrimination capacity and its utility for risk stratification. Lastly, future modifications of the model relying on the uncalibrated radial BP should be performed to overcome a possible systematic error evidenced at higher CO values that are often observed in athletes. This error might be attributed to the limited number of higher CO values in the *in silico* population.

Conclusion

In this study, we described and validated an ANN-based methodology that allows for the non-invasive estimation of CO from a calibrated or uncalibrated radial BP waveform. This study was motivated by the fact that such a model would be of great value for easy and continuous CO monitoring in everyday life, optimizing patient management. The evaluation of the hypothesis that the uncalibrated radial BP waveform contains sufficient information

for accurately deriving CO was found to be true in a large *in silico* population of virtual subjects. We plan to investigate the validity of our results using *in vivo* human data. The latter will verify the clinical utility of the proposed model, while it will enable research applications for the integration of the model in wearable sensing systems, such as smartwatches or other consumer devices.

Data availability statement

The raw data supporting the conclusion of this article will be made available by the authors, without undue reservation.

Author contributions

VB conceived and designed the experiments. VB developed the original algorithms, analyzed the data, ran the experiments, and drafted the manuscript. All authors contributed to the article and approved the submitted version.

References

- Baek, H. J., Lee, H. B., Kim, J. S., Choi, J. M., Kim, K. K., and Haet, B. L. (2009). "Noninvasive biological signal monitoring in a car to evaluate a driver's stress and health state." *Telemedicine E-Health* 15 (2): 182–189. doi:10.1089/tmj.2008.0090
- Berkenstadt, H., Margalit, N., Hadani, M., Friedman, Z., Segal, E., Villa, Y., et al. (2001). Stroke volume variation as a predictor of fluid responsiveness in patients undergoing brain surgery. *Anesth. Analgesia* 92 (4), 984–989. doi:10.1097/00000539-200104000-00034
- Bikia, V. (2021). *Non-invasive monitoring of key hemodynamical and cardiac parameters using physics-based modelling and artificial intelligence*. doi:10.5075/EPFL-THESIS-9179
- Bikia, V., Pagoulitou, S., Trachet, B., Soulis, D., Protogerou, A. D., Papaioannou, T. G., et al. (2020a). Noninvasive cardiac output and central systolic pressure from cuff-pressure and pulse wave velocity. *IEEE J. Biomed. Health Inf.* 24 (7), 1968–1981. doi:10.1109/JBHI.2019.2956604
- Bikia, V., Papaioannou, T. G., Pagoulitou, S., Rovas, G., Oikonomou, E., Siasos, G., et al. (2020b). Noninvasive estimation of aortic hemodynamics and cardiac contractility using machine learning. *Sci. Rep.* 10 (1), 15015. doi:10.1038/s41598-020-72147-8
- Bikia, V., Rovas, G., Pagoulitou, S., and Stergiopoulos, N. (2021). Determination of aortic characteristic impedance and total arterial compliance from regional pulse wave velocities using machine learning: An *in-silico* study. *Front. Bioeng. Biotechnol.* 9 (5), 649866. doi:10.3389/fbioe.2021.649866
- Bland, J. M., and Altman, D. G. (1986). Statistical methods for assessing agreement between two methods of clinical measurement. *Lancet (London, Engl.)* 1 (8476), 307–310. doi:10.1016/s0140-6736(86)90837-8
- Critchley, L. A. H., and Critchley, J. A. J. H. (1999). A meta-analysis of studies using bias and precision statistics to compare cardiac output measurement techniques. *J. Clin. Monit. Comput.* 15 (2), 85–91. doi:10.1023/A:1009982611386
- Critchley, L. A. H., Huang, L., and Zhang, J. (2014). Continuous cardiac output monitoring: What do validation studies tell us? *Curr. Anesthesiol. Rep.* 4 (3), 242–250. doi:10.1007/s40140-014-0062-9
- Gaddum, N. R., Alastruey, J., Beerbaum, P., Chowienczyk, P., and Schaeffter, T. (2013). A technical assessment of pulse wave velocity algorithms applied to non-invasive arterial waveforms. *Ann. Biomed. Eng.* 41 (12), 2617–2629. doi:10.1007/s10439-013-0854-y
- Ganter, M. T., Alhashemi, J. A., Al-Shabasy, A. M., Schmid, U. M., Shalabi, S. A., Badri, A. M., et al. (2016). Continuous cardiac output measurement by un-calibrated pulse wave analysis and pulmonary artery catheter in patients with septic shock. *J. Clin. Monit. Comput.* 30 (1), 13–22. doi:10.1007/s10877-015-9672-0
- Geddes, L. A., Voelz, M. H., Babbs, C. F., Bourland, J. D., and Tacker, W. A. (1981). Pulse transit time as an indicator of arterial blood pressure. *Psychophysiology* 18 (1), 71–74. doi:10.1111/j.1469-8986.1981.tb01545.x
- Harris, K. C., Benoit, G., Dionne, J., Feber, J., Cloutier, L., Zarnke, K. B., et al. (2016). Hypertension Canada's 2016 Canadian hypertension education program guidelines for

Funding

Open access funding by École Polytechnique Fédérale de Lausanne.

Conflict of interest

The authors declare that the research was conducted in the absence of any commercial or financial relationships that could be construed as a potential conflict of interest.

Publisher's note

All claims expressed in this article are solely those of the authors and do not necessarily represent those of their affiliated organizations, or those of the publisher, the editors and the reviewers. Any product that may be evaluated in this article, or claim that may be made by its manufacturer, is not guaranteed or endorsed by the publisher.

blood pressure measurement, diagnosis, and assessment of risk of pediatric hypertension. *Can. J. Cardiol.* 32 (5), 589–597. doi:10.1016/j.cjca.2016.02.075

Hickson, S. S., Butlin, M., Graves, M., Taviani, V., Alberto, P., McEniery, C. M., et al. (2010). "The relationship of age with regional aortic stiffness and diameter." *JACC Cardiovasc. Imaging* 3 (12): 1247–1255. doi:10.1016/j.jcmg.2010.09.016

Jansen, J. R. C., Schreuder, J. J., Mulier, J. P., Smith, N. T., Settels, J. J., and Wesseling, K. H. (2001). A comparison of cardiac output derived from the arterial pressure wave against thermodilution in cardiac surgery patients. *Br. J. Anaesth.* 87 (2), 212–222. doi:10.1093/bja/87.2.212

Kim, J., Park, J., Kim, K., Chee, Y., Lim, Y., and Park, K. (2007). Development of A Noninvasive blood pressure estimation system for computer users. *Telemedicine E-Health* 13 (1), 57–64. doi:10.1089/tmj.2006.0034

Kim, S., Scalzo, F., Bergsneider, M., Vespa, P., Martin, N., and Hu, X. (2012). Noninvasive intracranial pressure assessment based on a data-mining approach using a nonlinear mapping function. *IEEE Trans. Biomed. Eng.* 59 (3), 619–626. doi:10.1109/TBME.2010.2093897

Kingma, D. P., and Jimmy, B. (2017). *Adam: A method for stochastic optimization*. San Diego: US. Available at: <https://arxiv.org/pdf/1412.6980.pdf>.

Lees, N., Hamilton, M., and Rhodes, A. (2009). Clinical review: Goal-directed therapy in high risk surgical patients. *Crit. Care* 13 (5), 231. doi:10.1186/cc8039

Liao, Y., Thompson, C., Peterson, S., Mandrola, J., and Muhammad, S. B. (2019). The future of wearable technologies and remote monitoring in health care. *Am. Soc. Clin. Oncol. Educ. Book. Am. Soc. Clin. Oncol.* 39 (1), 115–121. Annual Meeting. doi:10.1200/EDBK_238919

Litton, E., and Morgan, M. (2012). The PiCCO monitor: A review. *Anaesth. Intensive Care* 40 (3), 393–408. doi:10.1177/0310057X1204000304

Liu, F., Tsang, R. C. C., Jones, A. Y. M., Zhou, M., Xue, K., Chen, M., et al. (2021). Cardiodynamic variables measured by impedance cardiography during a 6-minute walk test are reliable predictors of peak oxygen consumption in young healthy adults. *PLOS ONE* 16 (5), e0252219. doi:10.1371/journal.pone.0252219

McKinney, W. (2010). "Data structures for statistical computing in Python," in Proceedings of the 9th Python in Science Conference, 51–56. doi:10.25080/Majora-92bf1922-00a

Nye, E. R. (1964). The effect of blood pressure alteration on the pulse wave velocity. *Heart* 26 (2), 261–265. doi:10.1136/hrt.26.2.261

O'Brien, E., Parati, G., George, S., Roland, A., Beilin, L., Bilo, G., et al. (2013). European society of hypertension position paper on ambulatory blood pressure monitoring. *J. Hypertens* 31 (9), 1731–1768. doi:10.1097/HJH.0b013e328363e964

Olipant, T. E. (2006). *A guide to NumPy*. Trelgol Publishing USA. Available at: https://scholar.google.com/citations?view_op=view_citation&hl=en&user=kUTSKZwAAAAJ&citation_for_view=kUTSKZwAAAAJ:qjMakFHDy7sC.

Parati, G., George, S., O'Brien, E., Roland, A., Lawrence, B., Bilo, G., et al. (2014). European society of hypertension practice guidelines for ambulatory blood pressure monitoring. *J. Hypertens.* 32 (7), 1359–1366. doi:10.1097/HJH.0000000000000221

- Pedregosa, F., Varoquaux, G., Gramfort, A., Michel, V., Thirion, B., Grisel, O., et al. (2011). *Scikit-Learn: Machine learning in Python* 12: 2825–30.
- Reymond, P., Merenda, F., Perren, F., Rüfenacht, D., and Stergiopoulos, N. (2009). Validation of a one-dimensional model of the systemic arterial tree. *Am. J. Physiology Heart Circulatory Physiology* 297 (1), H208–H222. doi:10.1152/ajpheart.00037.2009
- Saugel, B., Kouz, K., Scheeren, T. W. L., Greiwe, G., Hoppe, P., Romagnoli, S., et al. (2021). Cardiac output estimation using pulse wave analysis—physiology, algorithms, and technologies: A narrative review. *Br. J. Anaesth.* 126 (1), 67–76. doi:10.1016/j.bja.2020.09.049
- Segers, P., Rietzschel, E. R., MarcDe Buyzere, L., Vermeersch, S. J., Dirk De BacquerVan Bortel, L. M., De Backer, G., et al. (2007). Noninvasive (input) impedance, pulse wave velocity, and wave reflection in healthy middle-aged men and women. *Hypertension* 49 (6), 1248–1255. doi:10.1161/HYPERTENSIONAHA.106.085480
- Stephens, A., Smulyan, H., and Gribbin, B. (1976). Pulse wave velocity and blood pressure change: Calibration and applications. *Psychophysiology* 13 (5), 488–493. doi:10.1111/j.1469-8986.1976.tb00866.x
- Sun, J. X., Reisner, A. T., Saeed, M., and Mark, R. G. (2005). “Estimating cardiac output from arterial blood pressure waveforms: A critical evaluation using the mimic II database.” In *Computers in cardiology*, 295–298. Lyon, France: IEEE. doi:10.1109/CIC.2005.1588095
- Tzourio, C., Olivier, H., Godin, O., Soumaré, A., and Dufouil, C. (2017). Impact of home blood pressure monitoring on blood pressure control in older individuals: A French randomized study. *J. Hypertens.* 35 (3), 612–620. doi:10.1097/HJH.0000000000001191
- Udy, A. A., Altukroni, M., Jarett, P., Roberts, J. A., and Lipman, J. (2012). A comparison of pulse contour wave analysis and ultrasonic cardiac output monitoring in the critically ill. *Anaesth. Intensive Care* 40 (4), 631–637. doi:10.1177/0310057x1204000408
- Zinoveev, A., Castro, J. M., García-Espinosa, V., Marin, M., Chiesa, P., Bia, D., et al. (2019). Aortic pressure and forward and backward wave components in children, adolescents and young-adults: Agreement between brachial oscillometry, radial and carotid tonometry data and analysis of factors associated with their differences. *PLOS ONE* 14 (12), e0226709. doi:10.1371/journal.pone.0226709
- Zócalo, Y., Yanina, V., García-Espinosa, V., Castro, J. M., Zinoveev, A., Marin, M., et al. (2021). Stroke volume and cardiac output non-invasive monitoring based on brachial oscillometry-derived pulse contour analysis: Explanatory variables and reference intervals throughout life (3–88 Years). *Cardiol. J.* 28 (6), 864–878. doi:10.5603/CJ.a2020.0031